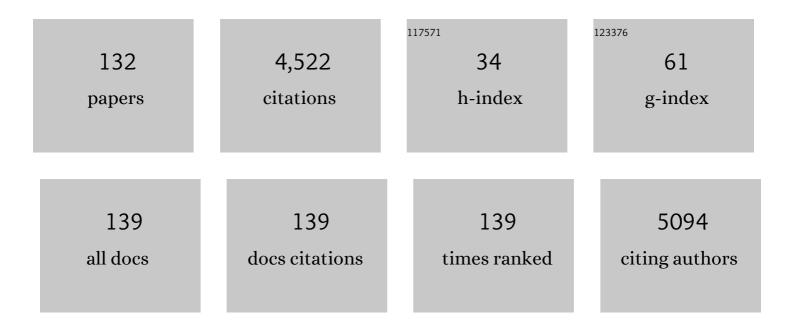
Jim Pfaendtner

List of Publications by Year in descending order

Source: https://exaly.com/author-pdf/826440/publications.pdf Version: 2024-02-01



IIM DEAENDTHED

#	Article	IF	CITATIONS
1	The General AMBER Force Field (GAFF) Can Accurately Predict Thermodynamic and Transport Properties of Many Ionic Liquids. Journal of Physical Chemistry B, 2015, 119, 5882-5895.	1.2	319
2	Efficient Sampling of High-Dimensional Free-Energy Landscapes with Parallel Bias Metadynamics. Journal of Chemical Theory and Computation, 2015, 11, 5062-5067.	2.3	182
3	Ice-nucleating bacteria control the order and dynamics of interfacial water. Science Advances, 2016, 2, e1501630.	4.7	182
4	The 1-D hindered rotor approximation. Theoretical Chemistry Accounts, 2007, 118, 881-898.	0.5	168
5	A Systematic Methodology for Defining Coarse-Grained Sites in Large Biomolecules. Biophysical Journal, 2008, 95, 5073-5083.	0.2	153
6	Trimethylamine <i>N</i> -oxide–derived zwitterionic polymers: A new class of ultralow fouling bioinspired materials. Science Advances, 2019, 5, eaaw9562.	4.7	149
7	Systematic Multiscale Parameterization of Heterogeneous Elastic Network Models of Proteins. Biophysical Journal, 2008, 95, 4183-4192.	0.2	148
8	Efficient Simulation of Explicitly Solvated Proteins in the Well-Tempered Ensemble. Journal of Chemical Theory and Computation, 2012, 8, 2189-2192.	2.3	127
9	Nucleotide-dependent conformational states of actin. Proceedings of the National Academy of Sciences of the United States of America, 2009, 106, 12723-12728.	3.3	106
10	Exhaustively Sampling Peptide Adsorption with Metadynamics. Langmuir, 2013, 29, 7999-8009.	1.6	103
11	Deconstruction of high-density polyethylene into liquid hydrocarbon fuels and lubricants by hydrogenolysis over Ru catalyst. Chem Catalysis, 2021, 1, 437-455.	2.9	101
12	Actin filament remodeling by actin depolymerization factor/cofilin. Proceedings of the National Academy of Sciences of the United States of America, 2010, 107, 7299-7304.	3.3	100
13	Lexicography of kinetic modeling of complex reaction networks. AICHE Journal, 2005, 51, 2112-2121.	1.8	92
14	Millisecond Pulsed Films Unify the Mechanisms of Cellulose Fragmentation. Chemistry of Materials, 2016, 28, 3108-3114.	3.2	87
15	Structure and Dynamics of the Actin Filament. Journal of Molecular Biology, 2010, 396, 252-263.	2.0	84
16	Structure, Dynamics, and Activity of Xylanase Solvated in Binary Mixtures of Ionic Liquid and Water. ACS Chemical Biology, 2013, 8, 1179-1186.	1.6	84
17	Defining Coarse-Grained Representations of Large Biomolecules and Biomolecular Complexes from Elastic Network Models. Biophysical Journal, 2009, 97, 2327-2337.	0.2	82
18	Ab Initio Study of Acrylate Polymerization Reactions: Methyl Methacrylate and Methyl Acrylate Propagation. Journal of Physical Chemistry A, 2008, 112, 6772-6782.	1.1	73

Jim Pfaendtner

#	Article	IF	CITATIONS
19	Data science: Accelerating innovation and discovery in chemical engineering. AICHE Journal, 2016, 62, 1402-1416.	1.8	63
20	Comparison of Three Ionic Liquid-Tolerant Cellulases by Molecular Dynamics. Biophysical Journal, 2015, 108, 880-892.	0.2	62
21	Application of machine learning to pyrolysis reaction networks: Reducing model solution time to enable process optimization. Computers and Chemical Engineering, 2017, 104, 56-63.	2.0	61
22	Quantum Chemical Investigation of Low-Temperature Intramolecular Hydrogen Transfer Reactions of Hydrocarbons. Journal of Physical Chemistry A, 2006, 110, 10863-10871.	1.1	60
23	Mechanistic Modeling of Lubricant Degradation. 1. Structureâ îReactivity Relationships for Free-Radical Oxidation. Industrial & Engineering Chemistry Research, 2008, 47, 2886-2896.	1.8	57
24	Diatom Mimics: Directing the Formation of Biosilica Nanoparticles by Controlled Folding of Lysine-Leucine Peptides. Journal of the American Chemical Society, 2014, 136, 15134-15137.	6.6	54
25	Structural and Dynamic Features of Candida rugosa Lipase 1 in Water, Octane, Toluene, and Ionic Liquids BMIM-PF6 and BMIM-NO3. Journal of Physical Chemistry B, 2013, 117, 2662-2670.	1.2	53
26	Mechanistic Modeling of Lubricant Degradation. 2. The Autoxidation of Decane and Octane. Industrial & Engineering Chemistry Research, 2008, 47, 2897-2904.	1.8	51
27	Molecular dynamics investigation of the ionic liquid/enzyme interface: Application to engineering enzyme surface charge. Proteins: Structure, Function and Bioinformatics, 2015, 83, 670-680.	1.5	50
28	New Approach for Investigating Reaction Dynamics and Rates with Ab Initio Calculations. Journal of Physical Chemistry A, 2016, 120, 299-305.	1.1	44
29	Enhanced sampling of chemical and biochemical reactions with metadynamics. Molecular Simulation, 2015, 41, 55-72.	0.9	41
30	Free Energy of Solvated Salt Bridges: A Simulation and Experimental Study. Journal of Physical Chemistry B, 2013, 117, 7254-7259.	1.2	40
31	Detailed Kinetic Modeling of Lignin Pyrolysis for Process Optimization. Industrial & Engineering Chemistry Research, 2016, 55, 9147-9153.	1.8	40
32	lce-nucleating proteins are activated by low temperatures to control the structure of interfacial water. Nature Communications, 2021, 12, 1183.	5.8	40
33	Folding and insertion thermodynamics of the transmembrane WALP peptide. Journal of Chemical Physics, 2015, 143, 243127.	1.2	37
34	Fast Pyrolysis of Wood for Biofuels: Spatiotemporally Resolved Diffuse Reflectance Inâ€situ Spectroscopy of Particles. ChemSusChem, 2014, 7, 765-776.	3.6	35
35	Strong Electrostatic Interactions Lead to Entropically Favorable Binding of Peptides to Charged Surfaces. Langmuir, 2016, 32, 5690-5701.	1.6	35
36	The Structure of the Diatom Silaffin Peptide R5 within Freestanding Twoâ€Dimensional Biosilica Sheets. Angewandte Chemie - International Edition, 2017, 56, 8277-8280.	7.2	34

#	Article	IF	CITATIONS
37	Attention-based generative models for <i>de novo</i> molecular design. Chemical Science, 2021, 12, 8362-8372.	3.7	34
38	Structural Effects of Methionine Oxidation on Isolated Subdomains of Human Fibrin D and αC Regions. PLoS ONE, 2014, 9, e86981.	1.1	33
39	Biomimetic Growth of Ultrathin Silica Sheets Using Artificial Amphiphilic Peptides. Advanced Materials Interfaces, 2015, 2, 1500282.	1.9	33
40	Molecular Driving Forces in Peptide Adsorption to Metal Oxide Surfaces. Langmuir, 2019, 35, 5911-5920.	1.6	33
41	Car–Parrinello Molecular Dynamics + Metadynamics Study of High-Temperature Methanol Oxidation Reactions Using Generic Collective Variables. Journal of Physical Chemistry C, 2014, 118, 10764-10770.	1.5	31
42	Kinetics and mechanism of ionic-liquid induced protein unfolding: application to the model protein HP35. Molecular Systems Design and Engineering, 2016, 1, 382-390.	1.7	31
43	Essential slow degrees of freedom in protein-surface simulations: A metadynamics investigation. Biochemical and Biophysical Research Communications, 2018, 498, 274-281.	1.0	30
44	Orientation and Conformation of Proteins at the Air–Water Interface Determined from Integrative Molecular Dynamics Simulations and Sum Frequency Generation Spectroscopy. Langmuir, 2020, 36, 11855-11865.	1.6	30
45	Key Structural Features of the Actin Filament Arp2/3 Complex Branch Junction Revealed by Molecular Simulation. Journal of Molecular Biology, 2012, 416, 148-161.	2.0	29
46	Investigating the Role of Phosphorylation in the Binding of Silaffin Peptide R5 to Silica with Molecular Dynamics Simulations. Langmuir, 2018, 34, 1199-1207.	1.6	29
47	Effect of Hydrophobic and Hydrophilic Surfaces on the Stability of Double-Stranded DNA. Biomacromolecules, 2015, 16, 1862-1869.	2.6	28
48	Trp-Cage Folding on Organic Surfaces. Journal of Physical Chemistry B, 2015, 119, 10417-10425.	1.2	28
49	Solvatochromism and Conformational Changes in Fully Dissolved Poly(3-alkylthiophene)s. Langmuir, 2015, 31, 458-468.	1.6	28
50	Peptoid Backbone Flexibilility Dictates Its Interaction with Water and Surfaces: A Molecular Dynamics Investigation. Biomacromolecules, 2018, 19, 1006-1015.	2.6	28
51	Statistical models are able to predict ionic liquid viscosity across a wide range of chemical functionalities and experimental conditions. Molecular Systems Design and Engineering, 2018, 3, 253-263.	1.7	28
52	MARTINI-Compatible Coarse-Grained Model for the Mesoscale Simulation of Peptoids. Journal of Physical Chemistry B, 2020, 124, 7745-7764.	1.2	28
53	Ultrafast Reorientational Dynamics of Leucine at the Air–Water Interface. Journal of the American Chemical Society, 2016, 138, 5226-5229.	6.6	26
54	Destabilization of Human Serum Albumin by Ionic Liquids Studied Using Enhanced Molecular Dynamics Simulations. Journal of Physical Chemistry B, 2016, 120, 12079-12087.	1.2	26

#	Article	IF	CITATIONS
55	Generic Biphasic Catalytic Approach for Producing Renewable Diesel from Fatty Acids and Vegetable Oils. ACS Catalysis, 2019, 9, 3753-3763.	5.5	25
56	Lifting the Curse of Dimensionality on Enhanced Sampling of Reaction Networks with Parallel Bias Metadynamics. Journal of Chemical Theory and Computation, 2018, 14, 2516-2525.	2.3	24
57	Ionic Liquids Can Selectively Change the Conformational Free-Energy Landscape of Sugar Rings. Journal of Chemical Theory and Computation, 2014, 10, 507-510.	2.3	23
58	Biasing Smarter, Not Harder, by Partitioning Collective Variables into Families in Parallel Bias Metadynamics. Journal of Chemical Theory and Computation, 2018, 14, 4985-4990.	2.3	23
59	Effect of Fluoroethylene Carbonate Additives on the Initial Formation of the Solid Electrolyte Interphase on an Oxygen-Functionalized Graphitic Anode in Lithium-Ion Batteries. ACS Applied Materials & Interfaces, 2021, 13, 8169-8180.	4.0	23
60	Elucidation of structure–reactivity relationships in hindered phenols via quantum chemistry and transition state theory. Chemical Engineering Science, 2007, 62, 5232-5239.	1.9	22
61	Chain Flexibility in Self-Assembled Monolayers Affects Protein Adsorption and Surface Hydration: A Molecular Dynamics Study. Journal of Physical Chemistry B, 2016, 120, 10423-10432.	1.2	22
62	Assessment of molecular dynamics simulations for amorphous poly(3-hexylthiophene) using neutron and X-ray scattering experiments. Soft Matter, 2019, 15, 5067-5083.	1.2	22
63	Characterizing the Catalyzed Hydrolysis of β-1,4 Glycosidic Bonds Using Density Functional Theory. Journal of Physical Chemistry A, 2013, 117, 14200-14208.	1.1	21
64	Elucidating sequence and solvent specific design targets to protect and stabilize enzymes for biocatalysis in ionic liquids. Physical Chemistry Chemical Physics, 2017, 19, 17426-17433.	1.3	21
65	Sequence–Structure–Binding Relationships Reveal Adhesion Behavior of the Car9 Solid-Binding Peptide: An Integrated Experimental and Simulation Study. Journal of the American Chemical Society, 2020, 142, 2355-2363.	6.6	21
66	Mechanism of Competitive Inhibition and Destabilization of <i>Acidothermus cellulolyticus</i> Endoglucanase 1 by Ionic Liquids. Journal of Physical Chemistry B, 2017, 121, 10793-10803.	1.2	20
67	Molecular Dynamics Simulation and Coarse-Grained Analysis of the Arp2/3 Complex. Biophysical Journal, 2008, 95, 5324-5333.	0.2	19
68	Quantifying the Molecular-Scale Aqueous Response to the Mica Surface. Journal of Physical Chemistry C, 2017, 121, 18496-18504.	1.5	19
69	Studies of Dynamic Binding of Amino Acids to TiO ₂ Nanoparticle Surfaces by Solution NMR and Molecular Dynamics Simulations. Langmuir, 2020, 36, 10341-10350.	1.6	19
70	Hierarchical Self-Assembly Pathways of Peptoid Helices and Sheets. Biomacromolecules, 2022, 23, 992-1008.	2.6	19
71	Enhancing the Oxidation of Toluene with External Electric Fields: a Reactive Molecular Dynamics Study. Scientific Reports, 2017, 7, 1710.	1.6	18
72	Assessing Generic Collective Variables for Determining Reaction Rates in Metadynamics Simulations. Journal of Chemical Theory and Computation, 2017, 13, 968-973.	2.3	17

#	Article	lF	CITATIONS
73	lce-binding site of surface-bound type III antifreeze protein partially decoupled from water. Physical Chemistry Chemical Physics, 2018, 20, 26926-26933.	1.3	17
74	Quantifying the Dynamics of Protein Self-Organization Using Deep Learning Analysis of Atomic Force Microscopy Data. Nano Letters, 2021, 21, 158-165.	4.5	17
75	Determining energy barriers and selectivities of a multi-pathway system with infrequent metadynamics. Journal of Chemical Physics, 2017, 146, 014108.	1.2	16
76	Lytic Polysaccharide Monooxygenases <i>Sc</i> LPMO10B and <i>Sc</i> LPMO10C Are Stable in Ionic Liquids As Determined by Molecular Simulations. Journal of Physical Chemistry B, 2016, 120, 3863-3872.	1.2	15
77	Solid-State NMR and MD Study of the Structure of the Statherin Mutant SNa15 on Mineral Surfaces. Journal of the American Chemical Society, 2019, 141, 1998-2011.	6.6	15
78	Diagnosing the Impact of External Electric Fields Chemical Kinetics: Application to Toluene Oxidation and Pyrolysis. Journal of Physical Chemistry A, 2019, 123, 3080-3089.	1.1	14
79	Elucidating Molecular Design Principles for Charge-Alternating Peptides. Biomacromolecules, 2020, 21, 435-443.	2.6	14
80	LK peptide side chain dynamics at interfaces are independent of secondary structure. Physical Chemistry Chemical Physics, 2017, 19, 28507-28511.	1.3	13
81	Solvent oligomerization pathways facilitated by electrolyte additives during solid-electrolyte interphase formation. Physical Chemistry Chemical Physics, 2020, 22, 21494-21503.	1.3	13
82	Design of Polyphosphate Inhibitors: A Molecular Dynamics Investigation on Polyethylene Glycol-Linked Cationic Binding Groups. Biomacromolecules, 2018, 19, 1358-1367.	2.6	12
83	Enhanced Activity and Stability of <i>Acidothermus cellulolyticus</i> Endoglucanase 1 in Ionic Liquids via Engineering Active Site Residues and Non-Native Disulfide Bridges. ACS Sustainable Chemistry and Engineering, 2020, 8, 11299-11307.	3.2	12
84	Continuous Molecular Representations of Ionic Liquids. Journal of Physical Chemistry B, 2020, 124, 8347-8357.	1.2	12
85	Acetylation dictates the morphology of nanophase biosilica precipitated by a 14â€amino acid leucine–lysine peptide. Journal of Peptide Science, 2017, 23, 141-147.	0.8	11
86	Amphiphilic peptide binding on crystalline vs. amorphous silica from molecular dynamics simulations. Molecular Physics, 2019, 117, 3642-3650.	0.8	11
87	Structure Characterization and Properties of Metal–Surfactant Complexes Dispersed in Organic Solvents. Langmuir, 2015, 31, 9006-9016.	1.6	10
88	Using Molecular Simulation to Study Biocatalysis in Ionic Liquids. Methods in Enzymology, 2016, 577, 419-441.	0.4	10
89	Closing the Gap Between Modeling and Experiments in the Self-Assembly of Biomolecules at Interfaces and in Solution. Chemistry of Materials, 2020, 32, 8043-8059.	3.2	10
90	Ion-dependent protein–surface interactions from intrinsic solvent response. Proceedings of the National Academy of Sciences of the United States of America, 2021, 118, .	3.3	10

#	Article	IF	CITATIONS
91	Predictive Theoretical Framework for Dynamic Control of Bioinspired Hybrid Nanoparticle Self-Assembly. ACS Nano, 2022, 16, 1919-1928.	7.3	10
92	Data Science in Chemical Engineering: Applications to Molecular Science. Annual Review of Chemical and Biomolecular Engineering, 2021, 12, 15-37.	3.3	9
93	Tribological degradation of two vegetableâ€based lubricants at elevated temperatures. Journal of Synthetic Lubrication: Research, Development and Application of Synthetic Lubricants and Functional Fluids, 2007, 24, 167-179.	0.7	8
94	Effect of an ionic liquid/air Interface on the structure and dynamics of amphiphilic peptides. Journal of Molecular Liquids, 2017, 236, 404-413.	2.3	8
95	Metadynamics to Enhance Sampling in Biomolecular Simulations. Methods in Molecular Biology, 2019, 2022, 179-200.	0.4	8
96	Impact of glutamate carboxylation in the adsorption of the α-1 domain of osteocalcin to hydroxyapatite and titania. Molecular Systems Design and Engineering, 2020, 5, 620-631.	1.7	8
97	Molecular recognition and specificity of biomolecules to titanium dioxide from molecular dynamics simulations. Npj Computational Materials, 2020, 6, .	3.5	8
98	Fantastic Liquids and Where To Find Them: Optimizations of Discrete Chemical Space. Journal of Chemical Information and Modeling, 2019, 59, 2617-2625.	2.5	7
99	Trimethylation of the R5 Silicaâ€Precipitating Peptide Increases Silica Particle Size by Redirecting Orthosilicate Binding. ChemBioChem, 2020, 21, 3208-3211.	1.3	7
100	Formulation and Efficacy of Catalase-Loaded Nanoparticles for the Treatment of Neonatal Hypoxic-Ischemic Encephalopathy. Pharmaceutics, 2021, 13, 1131.	2.0	6
101	Composition of Oxygen Functional Groups on Graphite Surfaces. Journal of Physical Chemistry C, 2022, 126, 10653-10667.	1.5	6
102	Molecular Driving Force for Facet Selectivity of Sequence-Defined Amphiphilic Peptoids at Au–Water Interfaces. Journal of Physical Chemistry B, 2022, 126, 5117-5126.	1.2	6
103	Determining dominant driving forces affecting controlled protein release from polymeric nanoparticles. Biointerphases, 2017, 12, 02D412.	0.6	5
104	Density functional tight-binding and infrequent metadynamics can capture entropic effects in intramolecular hydrogen transfer reactions. Journal of Chemical Physics, 2018, 148, 154101.	1.2	5
105	Elucidating the Molecular Interactions between Uremic Toxins and the Sudlow II Binding Site of Human Serum Albumin. Journal of Physical Chemistry B, 2020, 124, 3922-3930.	1.2	5
106	Probing the Thermodynamics and Kinetics of Ethylene Carbonate Reduction at the Electrode-Electrolyte Interface with Molecular Simulations. Journal of Chemical Physics, 2021, 155, 204703.	1.2	5
107	Peptoidâ€Directed Formation of Fiveâ€Fold Twinned Au Nanostars through Particle Attachment and Facet Stabilization. Angewandte Chemie - International Edition, 2022, 61, .	7.2	5
108	Contraâ€ŧhermodynamic Behavior in Intermolecular Hydrogen Transfer of Alkylperoxy Radicals. ChemPhysChem, 2007, 8, 1969-1978.	1.0	4

#	Article	IF	CITATIONS
109	Assessing the Performance of Various Stochastic Optimization Methods on Chemical Kinetic Modeling of Combustion. Industrial & amp; Engineering Chemistry Research, 2020, 59, 19212-19225.	1.8	4
110	Efficient Sampling of High-Dimensional Free Energy Landscapes: A Review of Parallel Bias Metadynamics. Molecular Modeling and Simulation, 2021, , 123-141.	0.2	4
111	Analyzing the Long Time-Scale Dynamics of Uremic Toxins Bound to Sudlow Site II in Human Serum Albumin. Journal of Physical Chemistry B, 2021, 125, 2910-2920.	1.2	4
112	Effect of graphitic anode surface functionalization on the structure and dynamics of electrolytes at the interface. Journal of Chemical Physics, 2021, 155, 134702.	1.2	4
113	Membrane Structure of Aquaporin Observed with Combined Experimental and Theoretical Sum Frequency Generation Spectroscopy. Langmuir, 2021, 37, 13452-13459.	1.6	4
114	Optimization of Thermal Conductance at Interfaces Using Machine Learning Algorithms. ACS Applied Materials & Interfaces, 2022, 14, 32590-32597.	4.0	4
115	Thiolated Lysine‣eucine Peptides Selfâ€Assemble into Biosilica Nucleation Pits on Gold Surfaces. Advanced Materials Interfaces, 2017, 4, 1700399.	1.9	3
116	Redefining the Protein–Protein Interface: Coarse Graining and Combinatorics for an Improved Understanding of Amino Acid Contributions to the Protein–Protein Binding Affinity. Langmuir, 2017, 33, 11511-11517.	1.6	3
117	IL-Net: Using Expert Knowledge to Guide the Design of Furcated Neural Networks. , 2018, , .		3
118	Combining Molecular and Spin Dynamics Simulations with Solid-State NMR: A Case Study of Amphiphilic Lysine–Leucine Repeat Peptide Aggregates. Journal of Physical Chemistry B, 2019, 123, 10915-10929.	1.2	3
119	Direct Evidence for Aligned Binding of Cellulase Enzymes to Cellulose Surfaces. Journal of Physical Chemistry Letters, 2021, 12, 10684-10688.	2.1	3
120	Elucidating the role of catalytic amino acid residues in the peptide-mediated silica oligomerization reaction mechanism. Physical Chemistry Chemical Physics, 2022, 24, 3664-3674.	1.3	3
121	Exploring structure and dynamics of the polylacticâ€coâ€glycolic acid–polyethylene glycol copolymer and its homopolymer constituents in various solvents using allâ€atom molecular dynamics. Journal of Applied Polymer Science, 2022, 139, .	1.3	3
122	Inhibition of the Exoglucanase Cel7A by a Douglas-Fir-Condensed Tannin. Journal of Physical Chemistry B, 2018, 122, 8665-8674.	1.2	2
123	<i>The Journal of Physical Chemistry A</i> / <i>B</i> / <i>C</i> Virtual Special Issue on Machine Learning in Physical Chemistry B, 2020, 124, 9767-9772.	1.2	2
124	<i>The Journal of Physical Chemistry A</i> / <i>B</i> / <i>C</i> Virtual Special Issue on Machine Learning in Physical Chemistry A, 2020, 124, 9113-9118.	1.1	2
125	Substitution of distal and active site residues reduces product inhibition of E1 from <i>Acidothermus Cellulolyticus</i> . Protein Engineering, Design and Selection, 2021, 34, .	1.0	2
126	Peptoidâ€Directed Formation of Fiveâ€Fold Twinned Au Nanostars through Particle Attachment and Facet Stabilization. Angewandte Chemie, 2022, 134, .	1.6	2

#	Article	IF	CITATIONS
127	<i>The Journal of Physical Chemistry A</i> / <i>B</i> / <i>C</i> Virtual Special Issue on Machine Learning in Physical Chemistry. Journal of Physical Chemistry C, 2020, 124, 24033-24038.	1.5	1
128	Peptide Mimic of the Marine Sponge Protein Silicatein Fabricates Ultrathin Nanosheets of Silicon Dioxide and Titanium Dioxide. Langmuir, 0, , .	1.6	1
129	Surface Assembly: Thiolated Lysineâ€Leucine Peptides Selfâ€Assemble into Biosilica Nucleation Pits on Gold Surfaces (Adv. Mater. Interfaces 16/2017). Advanced Materials Interfaces, 2017, 4, .	1.9	Ο
130	Coagulopathy In Trauma Patients Is Accompanied By Oxidation Of a Methionine Residue In The αC Domain Of Fibrinogen and Abnormal Fibrin Polymerization. Blood, 2013, 122, 1097-1097.	0.6	0
131	Theoretical Investigation of Organohalide Perovskite Degradation in Water. ECS Meeting Abstracts, 2021, MA2021-02, 636-636.	0.0	0
132	Frontispiz: Peptoidâ€Directed Formation of Fiveâ€Fold Twinned Au Nanostars through Particle Attachment and Facet Stabilization. Angewandte Chemie, 2022, 134, .	1.6	0